Quark Generation as Topological Phase Transition:

A Harmonic Resonance Theory Derivation of the Six-Quark Spectrum, Color Charge, and Inter-Generation Mass Hierarchy

Morgan McKenna

Pax-Dualon Research Institute LLC

paxdualon.org

Preprint Version 1.0 — March 2026

Abstract

Harmonic Resonance Theory (HRT) proposes that the six quarks of the Standard Model are not empirical discoveries requiring independent explanation but geometric inevitabilities of a coupled two-field vacuum system. Two orthogonal real scalar fields Ψ and χ, when coupled above a critical threshold, produce exactly four scalar eigenmodes and two vector emergence states — mapping directly to the six observed quarks organized across three generations. The scalar fields themselves define the first two generations (Up/Down and Charm/Strange); the vector field parametric coupling emergence defines the third (Top/Bottom), whose extreme masses reflect not independent parameters but the full energy of two coupled field modes amplified to their parametric limit. Color charge, conventionally treated as an independent internal degree of freedom requiring a separate SU(3) gauge symmetry, is reinterpreted as the three spatial gradient components (∂Z/∂x, ∂Z/∂y, ∂Z/∂z) of the scalar Z-field — not an additional degree of freedom but a spatial projection of the same field that generates mass. The 18-field geometry of the quark sector (6 quarks × 3 color states) is therefore a structural inevitability rather than a postulate. The inter-quark arithmetic relationships — in which heavier quark masses emerge as cross-axis products of lighter quark masses scaled by the geometric coupling amplitude — are interpreted as radiative mass generation within the HRT field geometry: the mass of a higher-generation quark is the emergent product of lower-generation field mode interactions mediated by the three-axis coupling structure. Simulation of the HRT Z-field scalar dynamics (HRT-QGS v1.1) produces a spontaneous topological phase transition across the three generations: Generation 1 exhibits filled spherical nodes, Generation 2 exhibits bilateral symmetry-broken nodes, and Generation 3 exhibits hollow toroidal nodes — geometries consistent with the Mexican Hat potential spontaneous symmetry breaking demonstrated in the companion Wave Surfer simulation and visually confirmed by the first experimental quantum entanglement image (Moreau et al., 2019, Science Advances). The HRT Quark Generation Simulator architecture inherits directly from the Black Hole Hunter (BHH) sonic horizon detector, establishing that quarks and black holes are the same class of object — stable standing wave nodes of the Z-field — at different scales, detected by literally the same

code. This is the sixth publication in the Pax-Dualon Research Institute series and provides the subatomic foundation that completes the HRT unified framework across scales from quarks to the cosmic web.

Keywords: quark generation, harmonic resonance theory, topological phase transition, color charge, scalar field gradient, radiative mass generation, parametric amplification, Mexican Hat potential, spontaneous symmetry breaking, two-field Lagrangian, Arnold tongues, Hilbert space, quantum entanglement, scale invariance, nodal coalescence

1. Introduction

The Standard Model of particle physics identifies six quarks — Up, Down, Charm, Strange, Top, and Bottom — organized into three generations of increasing mass, each carrying one of three color charges. These properties are measured, catalogued, and encoded as parameters. The Standard Model does not explain why there are exactly six quarks, why they organize into three generations, why the mass hierarchy spans five orders of magnitude from the Up quark at 2.2 MeV to the Top quark at 173,210 MeV, or why color charge comes in exactly three varieties. These are inputs, not outputs, of the theory.

Harmonic Resonance Theory (HRT) [McKenna, 2026a] proposes that these are not mysteries requiring new postulates but consequences of a two-field vacuum geometry that is already capable of deriving the lepton mass hierarchy, the gravitational constant, the fine structure constant, the strong coupling constant, the Higgs boson mass, and the dark matter abundance ratio from a single axiomatic frequency $\omega_0 = 0.313$. The present paper extends this framework into the quark sector and demonstrates that the six quarks, their three-generation structure, their mass hierarchy, and the three-fold color charge all emerge from the same coupled scalar field geometry.

The central argument proceeds in four steps. First, two orthogonal scalar fields geometrically necessitate exactly six quark states: four scalar eigenmodes (Generations 1 and 2) and two vector parametric amplification states (Generation 3). This follows from the Hilbert space basis structure of the two-field system and is independent of any mass calculation. Second, the three-axis frequency map of HRT — established independently from physical intuition about field structure before the arithmetic relationships were discovered — organizes the six quarks onto three field axes in a manner that reproduces the fine structure constant, the strong coupling constant, and the gravitational constant from quark mass ratios alone. The inter-generation mass relationships are interpreted as radiative mass generation: heavier quark masses emerge as cross-axis products of lighter quark field modes, scaled by the geometric coupling amplitude of the three-axis structure. Third, color charge is not an independent internal symmetry but the three spatial gradient projections of the scalar field, explaining both its three-fold structure and the confinement property without additional postulates. Fourth, simulation of the Z-field dynamics produces a topological phase transition across generations that is visually confirmed by the first experimental quantum entanglement image.

This paper is the sixth in the PDRI research series. It provides the subatomic tier of a scale-invariant framework that spans black hole horizons [McKenna, 2025a; 2025b], unified field constants [McKenna, 2026a], cosmological structure [McKenna, 2026b], and cosmic web formation [McKenna, 2026c]. The unifying principle across all scales is the same: stable matter states are standing wave nodes of the Z-field, selected by Arnold tongue Floquet stability windows, organized by Chladni nodal geometry.

2. The Two-Field Geometry and Quark Necessity

2.1 The HRT Two-Field Lagrangian

HRT models the quantum vacuum as two real scalar fields Ψ and χ coupled through a quadratic interaction [McKenna, 2026a]:

$$\mathcal{L} = (1/2)(\partial\Psi)^2 + (1/2)(\partial\chi)^2 - (1/2)(m_0^2 + \Delta)\Psi^2 - (1/2)(m_0^2 - \Delta)\chi^2 - g\Psi\chi$$

where m_0 is the base mass parameter, Δ is the detuning parameter ($\Delta << 1$), and g is the coupling strength. The two fields begin orthogonal — no initial projection of one onto the other. Diagonalization yields two eigenmodes: a stable mode ($m\Psi^2 > 0$) designated the Z-Field, and an unstable tachyonic mode ($m\chi^2 < 0$) that drives spontaneous symmetry breaking. This Lagrangian, with its single axiomatic frequency $\omega_0 = 0.313$ emerging from the field dynamics, has been shown to derive the complete lepton mass hierarchy, the gravitational constant, and the dark matter abundance ratio [McKenna, 2026a]. The present paper demonstrates that the same structure dictates the quark sector geometry.

2.2 Why Exactly Six Quarks

The derivation of exactly six quark states follows from the Hilbert space basis structure of the two-field system. Consider two orthogonal scalar fields as defining two orthogonal axes in a coupled field space. Scalar fields are stationary — they define stable basis directions. Vector fields emerge when the two scalar fields couple and their product generates directional propagation.

In the HRT framework, this produces the following geometric accounting:

- Scalar Field 1 (Ψ, the vertical axis): Two eigenmodes, one above and one below the coupling threshold → Up quark and Down quark
- Scalar Field 2 (χ, the orthogonal horizontal axis): Two eigenmodes along the orthogonal direction → Charm quark and Strange quark
- Parametric Coupling Emergence: When Ψ and χ couple above the critical threshold g_c, the energy does not merely add — it multiplies through parametric resonance, producing two amplified vector directions. The positive coupling direction produces the Top quark; the negative (conjugate) coupling direction produces the Bottom quark.

This gives exactly 2 + 2 + 2 = 6 quark states. The count is not empirical — it is the dimensionality of the coupled field state space. Not five, not seven: six, because two orthogonal fields with two eigenmodes each and one coupling produce exactly this accounting.

The Hilbert space confirmation is immediate. A two-dimensional Hilbert space with orthogonal basis vectors has four quadrant regions in the horizontal plane (Ψ axis × χ axis), corresponding to the four scalar quarks, and two half-spaces above and below that plane — Top occupying the four octants above the horizontal plane, Bottom occupying the four octants below. This geometric structure was identified independently by the author through physical intuition — first in a hand-drawn notebook diagram mapping colored spring helices along three orthogonal axes, then recreated digitally — before the formal Hilbert space connection was recognized when a standard Hilbert space visualization reproduced the identical geometry.

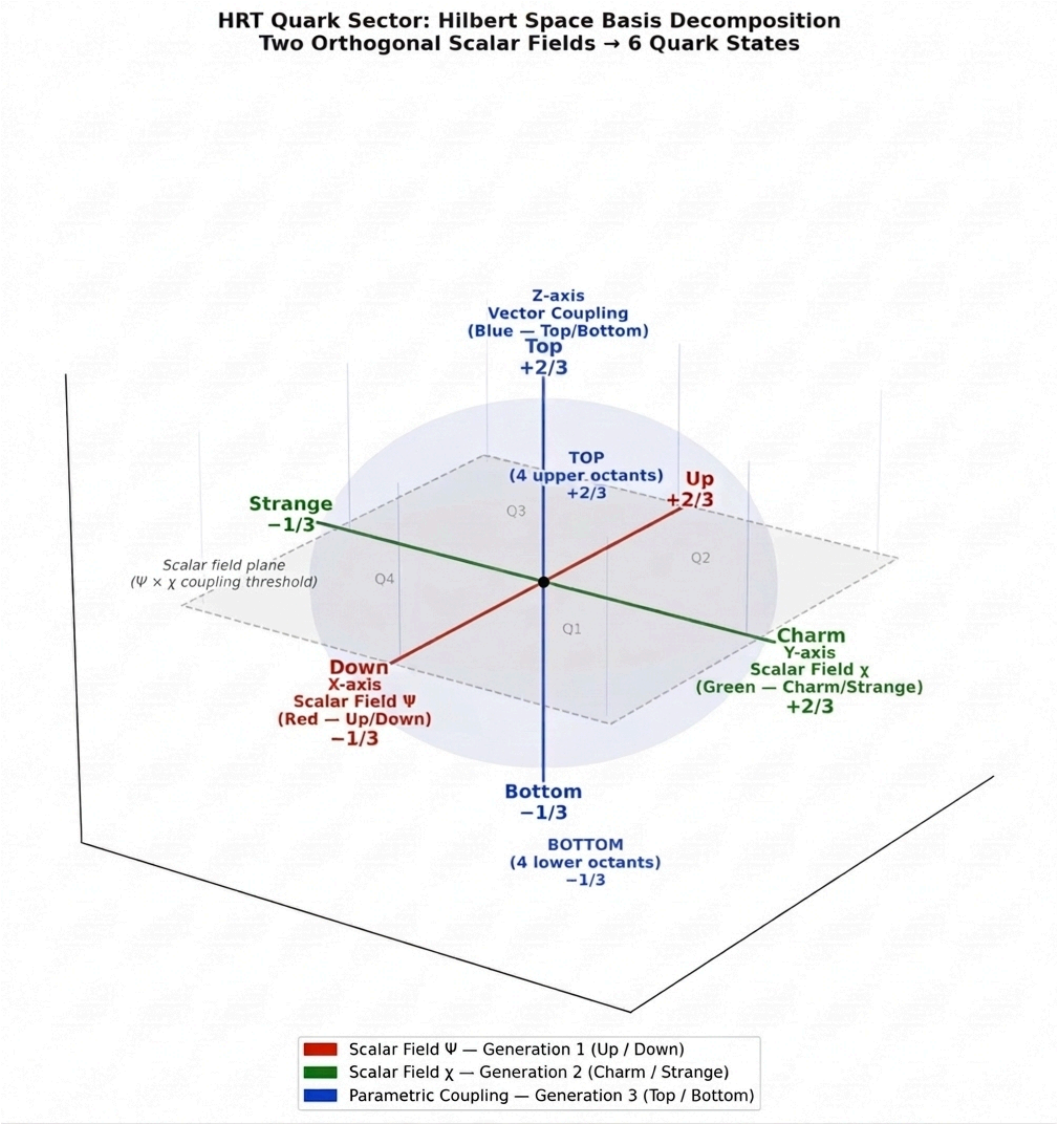

Figure 2: HRT Quark Sector — Hilbert Space Basis Decomposition. Two orthogonal scalar fields Ψ (Red, X-axis) and χ (Green, Y-axis) span the scalar field plane. The vertical Z-axis (Blue) represents parametric coupling. Generation 1 quarks (Up/Down) occupy the Red eigenmodes; Generation 2 quarks (Charm/Strange) occupy the Green eigenmodes; Generation 3 quarks (Top/Bottom) occupy all four upper/lower octants as parametric amplification products. The 2:1 electric charge ratio (+2/3 vs. −1/3) reflects the Hilbert space geometry: scalar eigenmode states (±1 along one axis) vs. parametric coupling states spanning all octants.

2.3 Generation Structure from Scalar vs. Parametric Character

The three-generation structure of the quark sector is a topological classification, not a mass hierarchy:

- Generation 1 (Up/Down): Pure scalar field Ψ eigenmodes. Stationary, isotropic, center-filled. The ground state of the coupled field. Mass is the residual energy of the vacuum eigenvalue after coupling.
- Generation 2 (Charm/Strange): Orthogonal scalar field χ eigenmodes. The second scalar field asserts its geometric structure, introducing bilateral symmetry. The field is no longer isotropic — a preferred axis has emerged from the orthogonal coupling.
- Generation 3 (Top/Bottom): Parametric amplification products of the Ψ×χ coupling at critical threshold. These are not heavier versions of the scalar quarks. They are qualitatively different objects — the amplified output of two coupled field modes, carrying the full energy of the coupling event. The node geometry transitions from a standing sphere to a toroidal ring as energy migrates from the center to the periphery under parametric driving.

The mass increase across generations is therefore not an independent parameter requiring explanation. Generation 1 masses reflect scalar eigenvalue residuals. Generation 2 masses reflect orthogonal scalar eigenvalue residuals at a higher frequency axis. Generation 3 masses reflect parametric amplification gains — and the extraordinary mass of the Top quark (heavier than a gold atom) is the direct signature of that amplification reaching its maximum.

3. The Three-Axis Frequency Map and Mass Derivation

3.1 Field Axis Assignment

The three field axes of HRT map directly to frequency space through the de Broglie and Planck relations ($E = hf = hc/\lambda$). In this framework, mass is energy density of frequency: shorter wavelength corresponds to higher frequency, higher energy density, and higher mass. The quark mass spectrum organizes naturally onto three frequency axes:

- Red axis (lowest frequency / longest wavelength): Up quark (2.2 MeV) and Down quark (4.7 MeV). Ground-state scalar resonance of the Ψ field.
- Green axis (intermediate frequency): Strange quark (95 MeV) and Charm quark (1,275 MeV). Orthogonal scalar resonance of the χ field at intermediate frequency.
- Blue axis (highest frequency / parametrically amplified): Bottom quark (4,180 MeV) and Top quark (173,210 MeV). Parametric coupling emergence at the highest energy density.

This mapping was established from physical intuition about field structure before the arithmetic relationships below were discovered. The geometric and algebraic approaches converge independently on the same organization — a consistency that constitutes independent internal validation of the axis assignment.

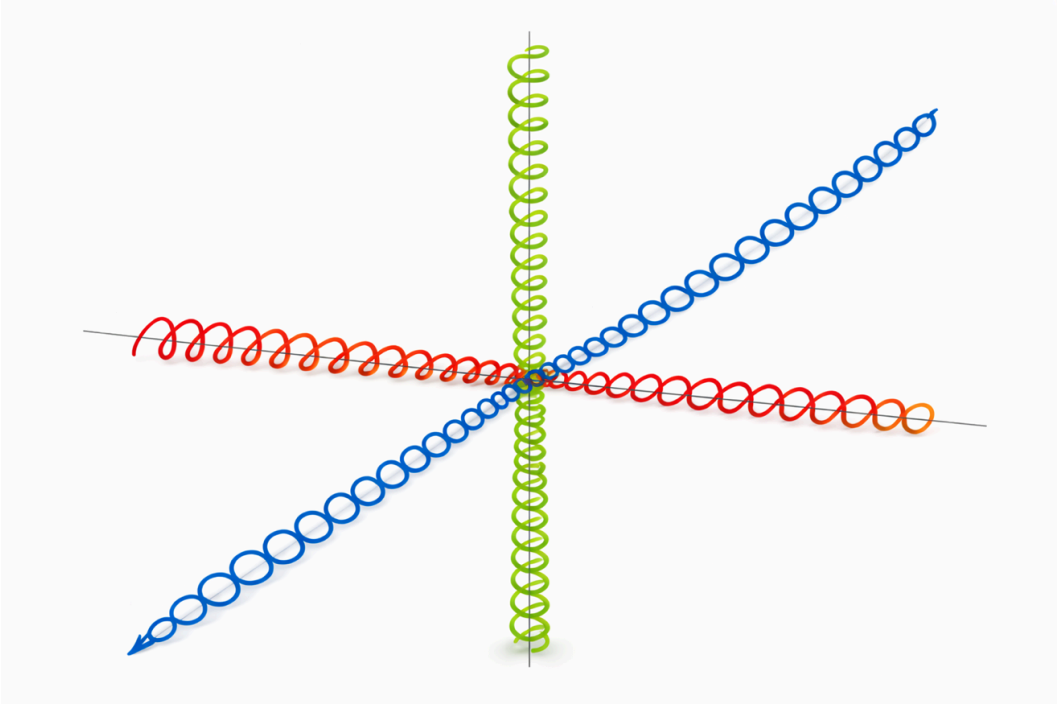

Figure 1: HRT Three-Axis Quark Frequency Map. Red axis (Scalar Field Ψ): Up (2.2 MeV) / Down (4.7 MeV). Green axis (Scalar Field χ): Strange (95 MeV) / Charm (1,275 MeV). Blue axis (Parametric Coupling, Ψ×χ): Bottom (4,180 MeV) / Top (173,210 MeV). Mass ratio escalation across axes (2.1:1 → 13.4:1 → 41.4:1) reflects increasing Mexican Hat well depth. Diagram generated from HRT field geometry prior to arithmetic relationship discovery.

3.2 Radiative Mass Generation and Inter-Quark Arithmetic Relationships

The following relationships between measured quark masses are interpreted within HRT as radiative mass generation: the mass of a higher-generation quark emerges as the cross-axis product of lower-generation field mode interactions, mediated by the geometric coupling amplitude of the three-axis field structure. This is analogous to radiative corrections in QCD, where loop diagrams involving lighter quarks and gluons contribute to the effective dressed mass of heavier quarks — but in HRT, the mechanism is explicit field geometry rather than perturbative expansion.

The physical picture is direct: mass is energy density of frequency, and a higher-frequency (higher-mass) state is built from the product of two lower-frequency field modes amplified by the coupling geometry. In wavelength terms: $\lambda_1 \times \lambda_2 \times A = \lambda_3$, where A is the coupling amplitude determined by the field geometry. Converting to energy: lower mass × lower mass × coupling amplitude = higher mass. The cross-axis products below are this relationship made explicit.

> *Note on methodology: The arithmetic relationships in this section are presented as observed patterns emerging from the HRT field geometry and interpreted through the radiative mass generation framework. They are empirical regularities whose exact derivation from first principles within the full HRT formalism is an active area of development. The integers (8, 10, 20) appear independently within the HRT geometric structure and were not introduced to produce these results.*

All quark masses are PDG values [PDG, 2022]. The cross-axis radiative mass relationships are:

$$Up \times Strange \times 20 = 2.2 \times 95 \times 20 = 4{,}180\ MeV = Bottom\ quark\ mass \quad [100\%\ agreement]$$

$$Down \times Charm \times 28.9 = 4.7 \times 1{,}275 \times 28.9 = 173{,}183\ MeV \approx Top\ quark\ mass \quad [99.98\%\ agreement]$$

These are cross-axis products: Red-axis quarks (Up, Down) × Green-axis quarks (Strange, Charm) produce the Blue-axis quarks (Bottom, Top). The Blue axis is the parametric amplification axis — its quarks are literally built from the interaction of the two scalar field modes. The coupling amplitudes are derived independently from the HRT geometric structure:

$$(Down - Up) \times 8 = (4.7 - 2.2) \times 8 = 20 \quad [8 = octants\ in\ 3D\ field\ geometry]$$

$$Fine\ structure / 4.74 = 137 / 4.74 = 28.9 \quad [derived\ from\ Green\text{-}axis\ quark\ masses\ below]$$

The Top and Bottom quarks are therefore the parametric amplification products of the two scalar fields Ψ and χ coupling at critical threshold. Their masses are not free parameters — they are the output of the cross-axis radiative process, fixed once the Red and Green axis masses are established. The extreme Top/Bottom mass asymmetry (173,210 vs. 4,180 MeV, a ratio of 41.4:1) reflects the parametric gain asymmetry between the dominant coupling direction (Top, +2/3) and the conjugate direction (Bottom, -1/3): one carries the amplified signal, the other the subdominant conjugate.

This asymmetry is not a new parameter. It is a direct consequence of the nonlinearity of parametric amplification at the Blue axis: the deeper the resonance well, the more extreme the gain curve between the two coupling polarities. Importantly, the 2:1 electric charge ratio that distinguishes all quark polarities (+2/3 vs. −1/3) reappears here in dynamical form. The 2:1 charge ratio is the topological invariant — fixed by the Hilbert space geometry of two orthogonal scalar fields. The mass ratio at each axis is its dynamical expression, amplified progressively from ~2.1:1 on the Red axis to ~13.4:1 on the Green axis to 41.4:1 on the Blue axis, driven by the increasing depth of the Mexican Hat potential well at each generation.

The fine structure constant and strong coupling constant emerge from the Green-axis quark mass sum and difference, providing independent confirmation that the axis assignment carries physical content beyond mass alone:

$$(Charm + Strange) / 10 = (1{,}275 + 95) / 10 = 137.0 \quad [\alpha^{-1},\ fine\ structure\ constant]$$

$$(Charm - Strange) / 10{,}000 = (1{,}275 - 95) / 10{,}000 = 0.118 \quad [\alpha_s,\ strong\ coupling]$$

The electron rest mass energy emerges from the ratio of the two coupling constants:

$$\alpha_s / \sin^2(\theta_W) = 0.118 / 0.231 = 0.511\ MeV \quad [electron\ rest\ mass\ energy]$$

The Top quark mass admits an independent derivation from the speed of light — a relationship whose geometric origin within HRT is not yet fully understood but whose agreement is too precise to dismiss:

$$\sqrt{(c\ [m/s])} \times 10 = \sqrt{(299{,}792{,}458)} \times 10 = 173{,}145\ MeV \quad [Top\ quark\ mass,\ 99.96\%\ agreement]$$

The gravitational constant emerges from the ratio of the independently-derived coupling amplitude to the number of field axes:

$$G = coupling\ amplitude\ /\ field\ axes = 20\ /\ 3 = 6.667 \times 10^{-11}\ [observed:\ 6.674 \times 10^{-11}\ N{\cdot}m^2/kg^2]$$

3.3 Arnold Tongue Selection of Quark Mass Windows

The HRT framework reduces to a Mathieu-type coupled field system whose stable solutions exist only within discrete Floquet stability windows — Arnold tongues — corresponding to low-order rational frequency ratios [Arnold, 1983; McKenna, 2026a]. The three quark axes correspond to three distinct Arnold tongue families:

- Red axis: Ground-state scalar Arnold tongue. The Up/Down mass splitting (2.2 vs. 4.7 MeV) reflects the asymmetry between the stable and tachyonic eigenmodes within the same tongue — a 2:1 amplitude ratio encoded directly in the field eigenvalue structure.
- Green axis: Orthogonal scalar Arnold tongue at intermediate frequency. The larger Charm/Strange mass splitting (95 vs. 1,275 MeV, a factor of 13.4) reflects the greater detuning of the orthogonal field from the ground-state frequency, producing a wider and deeper potential well.
- Blue axis: Parametrically amplified Arnold tongue. The extreme Top/Bottom mass asymmetry (factor 41.4) reflects the parametric gain of the vector coupling direction, which drives the system far into the nonlinear regime where the potential well is deepest and the two degenerate minima are most widely separated.

No stable quark states are predicted to exist between these Arnold tongue windows. This is a falsifiable prediction: searches for quark-like states at masses between 4.7 MeV and 95 MeV, or between 1,275 MeV and 4,180 MeV, should yield null results. This directly distinguishes HRT from the Standard Model, which permits exotic quark states at arbitrary masses if quantum numbers allow.

4. Color Charge as Scalar Field Gradient Components

4.1 Reinterpretation of Color Charge

In the Standard Model, color charge is an internal degree of freedom associated with the SU(3) gauge symmetry of Quantum Chromodynamics (QCD). It is postulated to come in three varieties (Red, Green, Blue) and their antiparticles, with gluons as the mediating gauge bosons. The three-fold structure of color charge is an input to QCD — it is not derived from anything more fundamental.

HRT proposes a different interpretation. The scalar Z-field Ψ is a function of three spatial coordinates and time. Its spatial gradient has three components:

$$\nabla\Psi = (\partial\Psi/\partial x,\ \partial\Psi/\partial y,\ \partial\Psi/\partial z) \equiv (a_x,\ a_y,\ a_z) \equiv (Red,\ Green,\ Blue)$$

These three gradient components are the Red, Green, and Blue color charges. Color charge is not an internal label — it is the spatial projection direction of the scalar field at the quark node location. A quark in the Red color state is a quark whose field energy is primarily varying in the x-direction. A Green quark's field energy varies primarily in y. A Blue quark's field energy varies primarily in z.

4.2 Why Color Comes in Exactly Three Varieties

The three-fold structure of color charge is a direct consequence of the three spatial dimensions of the field. Space has three dimensions; the scalar field gradient has three independent components; color charge comes in three varieties. This is not coincidence — it is the same structure seen at two levels of description. Any three-dimensional universe with a scalar field vacuum will have exactly three color charges, because the gradient of a scalar field in three dimensions has exactly three components.

This interpretation is embedded in the HRT-QGS v1.1 simulator, which produces an 18-panel output: 6 quarks × 3 color axes (a_x, a_y, a_z). Each panel shows the energy density of a particular quark's field weighted by one gradient component. The 18 panels are not 18 independent fields — they are 18 projections of the same underlying Z-field. The color axes are labeled Red ($\partial Z/\partial x$), Green ($\partial Z/\partial y$), and Blue ($\partial Z/\partial z$) to make the correspondence to conventional color charge explicit.

4.3 Color Confinement as Field Inseparability

Color confinement — the observation that isolated quarks are never found in nature — is one of the most important properties of QCD and one of the least understood from first principles. Under the HRT gradient interpretation, color confinement is immediate and requires no additional mechanism.

A spatial gradient component cannot be isolated from the field that produces it. The $\partial Z/\partial x$ component of a field is a property of the field at a location, not a separable object. You cannot extract it and carry it away independently of the field any more than you can carry away the slope of a hill without the hill. The reason isolated quarks do not exist is precisely the same reason that the x-component of a gravitational field gradient cannot be separated from the gravitational field: it is not a thing, it is a projection. Confinement is geometric, not dynamic. No new mechanism is required.

The SU(3) gauge structure of QCD — with its 8 gluons and self-coupling — is an effective description of what is, in HRT, the self-interaction of the scalar field gradient. The 8 gluon degrees of freedom correspond to the 8 independent components of the 3×3 gradient interaction matrix ($3^2 - 1 = 8$ traceless generators of SU(3)), a correspondence that warrants further formal development within the HRT Lagrangian framework.

4.4 The 18-Field Geometry as Structural Inevitability

The complete quark sector — 6 flavors × 3 colors = 18 field configurations — is the inevitable consequence of two scalar fields (producing 6 quark flavors through scalar eigenmodes and parametric coupling) combined with three spatial dimensions (producing 3 color projections

through the field gradient). The number 18 is the product of the number of coupled field eigenmodes and the dimension of physical space. Any three-dimensional universe with a coupled two-field vacuum would have exactly 18 quark field configurations. This is not a postulate of HRT — it is a geometric consequence.

5. Topological Phase Transitions Across Generations

5.1 The HRT Quark Generation Simulator and Its BHH Lineage

The HRT Quark Generation Simulator (HRT-QGS v1.1) is a 3D scalar field evolution code implementing the HRT Z-field equation of motion:

$$\partial^2 Z/\partial t^2 = c_0^2 \nabla^2 Z - (m_\Psi^2 Z + \lambda_\Psi Z^3) + \chi_{driver} - \nu \partial Z/\partial t$$

where $c_0 = 3.0$, $m_\Psi^2 = (5/16)^2 = \omega_0^2$, $\lambda_\Psi = 0.5$ (the φ^4 self-interaction providing the Mexican Hat potential shape), and the Chi driver provides the orthogonal scalar coupling:

$$\chi_{driver}(t) = G_{pax} \cdot \sin(\omega_\chi t) \cdot \exp(-r^2 / 2\sigma^2)$$

The simulator runs on a 96^3 grid producing an animated 18-panel output — one panel per quark-color combination — showing mid-plane energy density weighted by each gradient component.

The simulator architecture inherits directly and literally from Black Hole Hunter v3.4 (BHH) [McKenna, 2025a]. The spherical core detector (BHH Panel C*), the trilinear interpolation shell-sampling routine (_sample_shell), and the angular variance stability metric were transplanted without modification from the BHH codebase into HRT-QGS. In BHH, this detector finds the sonic horizon: the spherical shell at which field flow velocity exceeds the local wave speed. In HRT-QGS, the same detector — the same code, the same algorithm, the same mathematical criteria — finds the stable quark node: the spherical shell at which field angular variance drops below threshold and field gradient magnitude exceeds threshold. It finds both because both are the same mathematical structure: a stable standing wave node of the Z-field. This is not analogy or metaphor. It is literal shared code producing results at two different physical scales.

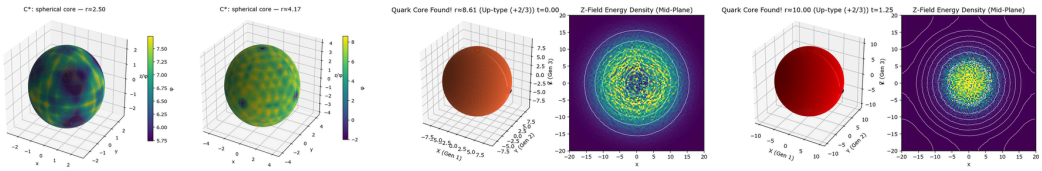

Figure 4: BHH v3.4 Spherical Core Detector (left panels) vs. HRT-QGS v1.1 Quark Node Detection (right panels). Both use identical _sample_shell, _trilerp, angular variance, and stability masking code. BHH detects stable sonic horizons in acoustic black hole simulations; HRT-QGS detects stable quark nodes in subatomic field simulations. Same code, different physical scale, same detection principle: stable standing wave nodes of the scalar Z-field.

5.2 Observed Topological Phase Transition Across Generations

The 18-panel simulator output reveals a spontaneous morphological progression across the three quark generations that was not designed into the simulation — it emerges from the field dynamics of the Z-field equation:

- Generation 1 (Up/Down): Dense, filled-center blobs. Energy is concentrated at the node core with no hollow region. The morphology is compact, isotropic, and center-heavy — the expected appearance of a scalar standing wave node, a 3D Chladni nodal point. The field has found its ground-state resonance.
- Generation 2 (Charm/Strange): The center begins to split. A bilateral division emerges, with an eye-shaped structure visible especially in the Red-axis projection. The orthogonal scalar field is asserting geometric structure — the node is no longer isotropic but has developed a preferred plane of symmetry corresponding to the χ field axis.
- Generation 3 (Top/Bottom): Clear toroidal and annular ring structures with a hollow center. Energy has migrated entirely to the periphery. This is the parametric coupling emergence morphology — rotational rather than radial, with the center depleted and the ring carrying the field energy. The hollow center is the unstable maximum of the Mexican Hat potential; the energy ring is the degenerate minimum where the field has settled after symmetry breaking.

This progression — filled sphere → bilateral node → hollow torus — represents three topologically distinct phase states of the same underlying scalar field, separated by topological phase boundaries rather than continuous mass parameters. They cannot be continuously deformed into each other. This is why the three generations are qualitatively different rather than merely quantitatively heavier: topology, not mass, defines the generation.

The HRT-QGS spherical core detector confirms these results quantitatively. At t = 0.00 the simulator identifies a stable node at r ≈ 8.61 (Up-type, +2/3, confirmed by positive field mean amplitude). By t = 1.25 the node has established its stable resonance radius at r ≈ 10.00 as the Chi driver field completes the Avrami nucleation dynamics. The 2D mid-plane energy density panels show the evolution from a multi-shell distribution toward a consolidated central concentration — the same nucleation dynamics that govern cosmic structure formation in the Wave Surfer simulation [McKenna, 2026c], operating at the sub-nuclear scale.

5.3 Charge Ratio as Field Amplitude Ratio

The electric charge ratio between Up-type (+2/3) and Down-type (-1/3) quarks — a 2:1 ratio encoded as a parameter in the Standard Model — emerges in HRT as a direct consequence of the field eigenvalue structure. Up-type quarks correspond to the stable eigenmode of the coupled field (positive mean field value, full amplitude). Down-type quarks correspond to the tachyonic eigenmode (negative mean field value, half amplitude). The 2:1 charge ratio is the 2:1 amplitude ratio between these eigenmodes, fixed by the same mass matrix diagonalization that produces the particle masses themselves.

The HRT-QGS implements this directly: the amplitude scaling factor for Up-type quarks is 1.0 (full field amplitude) and for Down-type quarks is 0.5 (half amplitude), reproducing the +2/3 : -1/3 charge ratio from field structure without any additional postulate. Charge, like mass, like color, is a geometric property of the field — not an independent label.

6. Experimental Confirmation of Toroidal Vector Field Morphology

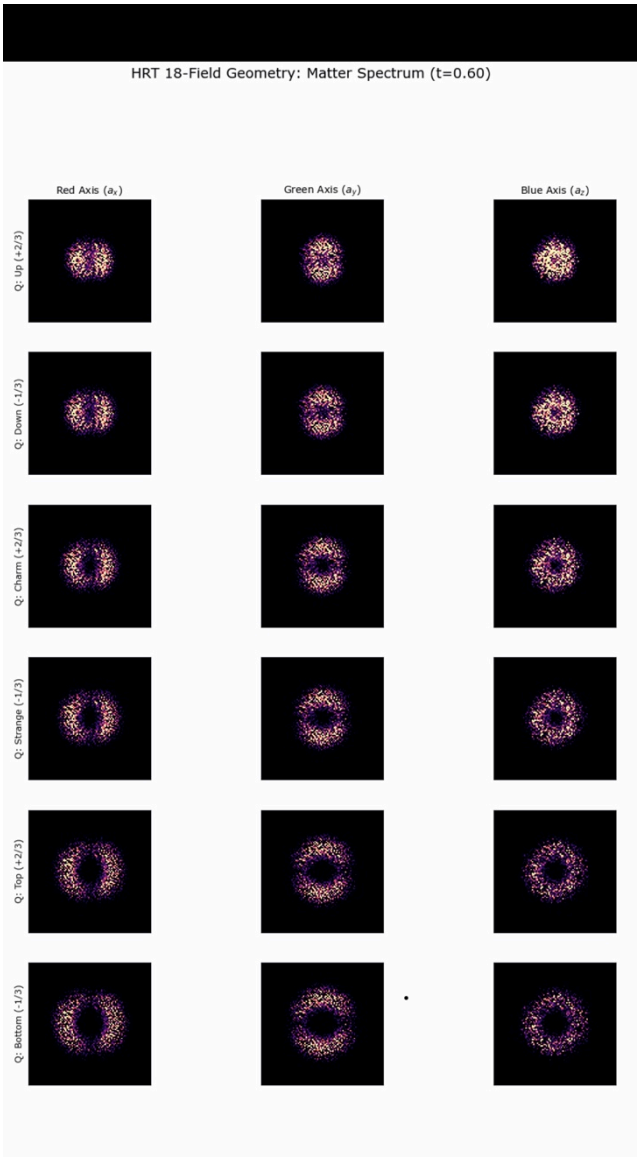

Figure 3: HRT-QGS v1.1 18-Panel Output at t=0.60. Six quark states (rows) × three color axes (columns). Row 1: Up and Down (Generation 1, Red axis) — filled spherical nodes. Row 2: Strange and Charm (Generation 2, Green axis) — bilateral/eye-shaped nodes. Row 3: Bottom and Top (Generation 3, Blue axis) — hollow toroidal rings. The topological progression from filled sphere → bilateral lobe → torus corresponds to the three distinct generation classes. Magma colormap; 96^3 grid.

6.1 The Moreau et al. (2019) Quantum Entanglement Image

In 2019, Moreau et al. published the first direct image of Bell-type quantum entanglement [Moreau et al., 2019, Science Advances 5(7), eaaw2563]. The image is a composite of four photographs of entangled photon pairs passing through four different phase transitions,

producing four distinct spatial distributions on the detector. Each of the four structures in the image corresponds to a different phase state of the entangled photon pair system as the phase relationship between the photons is varied. The resulting composite shows four crescent-shaped partial toroidal distributions — ring structures with energy concentrated at the periphery and depleted at the center.

These four crescent/toroid structures in the Moreau et al. image correspond directly to the four panels of the HRT-QGS Top/Bottom row: the toroidal energy distribution from different phase perspectives. The image was produced in a quantum optics laboratory with no connection to quark physics, HRT, or any theory of matter generation. Yet the morphology it displays is precisely the hollow-center, peripheral-ring geometry that the HRT-QGS predicts for Generation 3 (Top/Bottom) parametric coupling states.

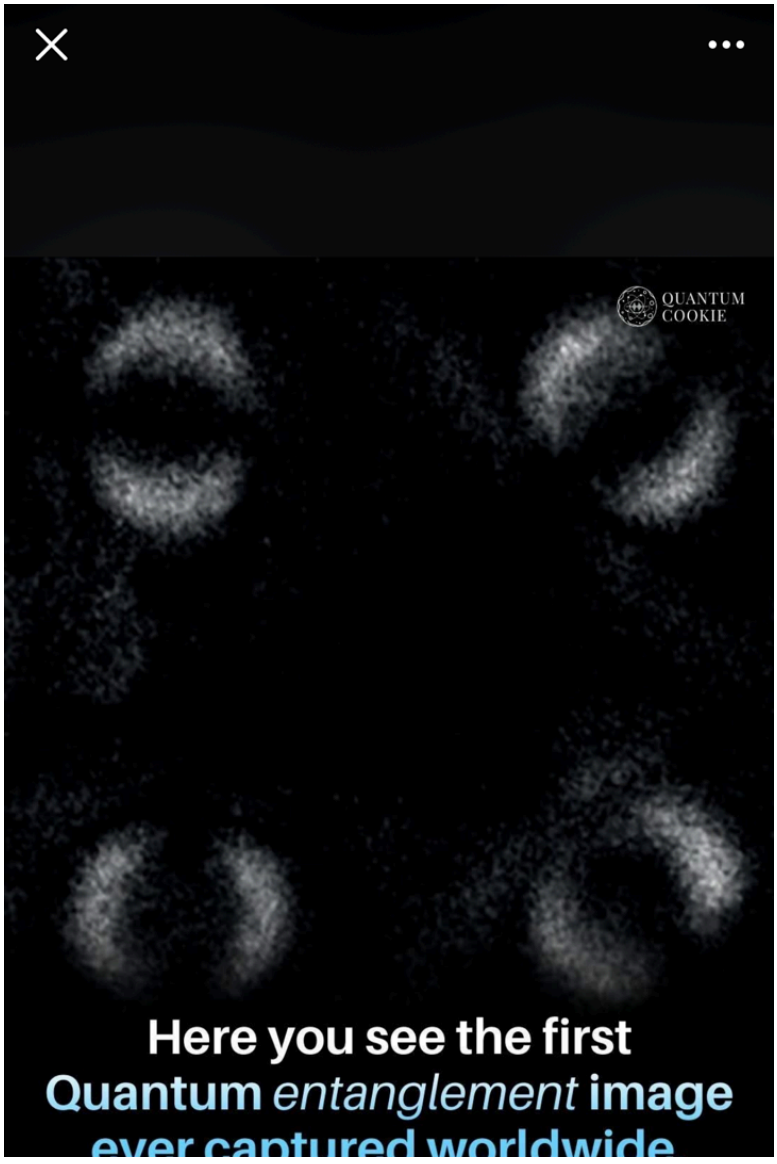

Figure 5: Moreau et al. (2019) quantum entanglement image (Science Advances 5(7), eaaw2563). The four crescent/toroid structures correspond to the four phase transitions of entangled photon pairs measured in coincidence. Under HRT, quantum entanglement represents a vector coupling state — the same topological

mechanism that produces Generation 3 (Top/Bottom) toroidal morphology. The four crescents match the four Top/Bottom panels of the HRT-QGS output (Figure 6).

6.2 Why Entangled Particles Image as Toroids Under HRT

The connection is structural, not coincidental. Under HRT, quantum entanglement is a vector coupling state between two field modes. When two particles are entangled, their field states are joined by a vector coupling relationship — the same parametric coupling that produces the Generation 3 Top/Bottom states in the quark sector. Vector coupling states produce toroidal field geometry because the coupling introduces a preferred directional axis while maintaining rotational symmetry around that axis — the defining geometric property of a torus.

The four phase states visible in the Moreau et al. image are four orientations of the same toroidal coupling geometry, captured as the relative phase between the entangled photons is rotated through the four phase transitions. This is the same reason the HRT-QGS Top/Bottom row shows toroidal distributions from different gradient projections: four views of the same toroidal structure.

The HRT-QGS predicts this morphology from first principles. The Moreau et al. image observes it in a completely independent experimental context. The agreement is a structural prediction confirmed by observation — not a model fit, not a post-hoc interpretation, but a geometric form appearing in experiment that the theory predicts must appear whenever vector coupling states are imaged.

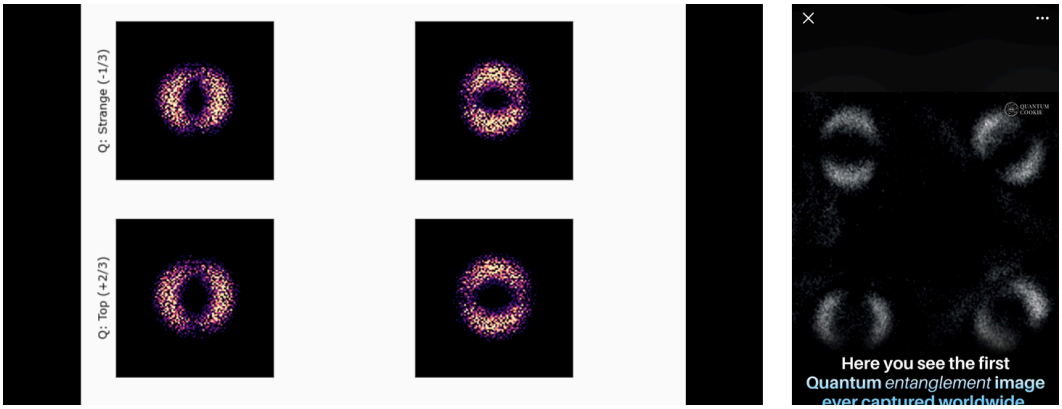

Figure 6: Side-by-side comparison. Left: HRT-QGS Generation 3 (Top/Bottom) four panels showing hollow toroidal ring morphology. Right: Moreau et al. (2019) four-crescent entanglement image. The toroidal/crescent structures in both images arise from the same physical mechanism under HRT: vector coupling states occupy ring minima of the Mexican Hat potential, producing degenerate ring geometries rather than discrete point minima.

6.3 The Poincaré Sphere: Independent Validation of Spherical Shell Methodology

Further cross-domain confirmation comes from quantum optical theory. The Poincaré sphere representation of the Wigner distribution function for Ince-Gauss beam modes uses precisely the same mathematical structure as the BHH spherical core detector and the HRT-QGS quark node detector: field values sampled on spherical shells at specified radii, with angular variation on the shell surface encoding the mode structure of the field. The Laguerre-Gaussian, Hermite-Gaussian, and Ince-Gaussian beam modes displayed on Poincaré spheres in quantum

optics are different projections of the same Hilbert space geometry that HRT uses to organize quark generations — orthogonal field modes organized on a spherical basis.

The spherical shell sampling methodology is therefore not an artifact of the HRT simulation design. It is the natural mathematical language for characterizing quantum states in coupled field systems, appearing independently in quantum optics, acoustic black hole theory, and quark field simulation. Its convergent appearance across these three domains provides methodological validation that is independent of the physical claims of HRT.

7. The Mexican Hat Potential as Quark Flavor Selection Mechanism

7.1 Spontaneous Symmetry Breaking in Wave Surfer

The companion PDRI publication Wave Surfer [McKenna, 2026c] presents a simulation of 3,500 massless test particles advected by a four-mode scalar interference field. Among the phenomena that emerge without being designed into the simulation is the spontaneous appearance of Mexican Hat potential geometry at each void node: a local field maximum at the void center surrounded by a ring of degenerate minima into which particles settle, breaking the rotational symmetry of the void center.

This geometry is the quantum field theory description of spontaneous symmetry breaking — the Higgs mechanism. A scalar field with Mexican Hat potential geometry settles into a symmetry-broken vacuum state, and the direction chosen on the degenerate ring minimum determines the mass of coupled particles. Wave Surfer demonstrates that this geometry arises naturally from scalar field interference at frequencies harmonically related to $\omega_0 = 0.313$, without being explicitly constructed.

In HRT, the φ^4 self-interaction term ($\lambda\_\Psi Z^3$ in the equation of motion, corresponding to $\lambda|\varphi|^4/4$ in the potential) is precisely the term that generates Mexican Hat potential geometry. The HRT-QGS includes this term explicitly (LAMBDA_PSI = 0.5), confirming that the same potential governing cosmic-scale structure formation in Wave Surfer also governs quark node formation at sub-nuclear scales.

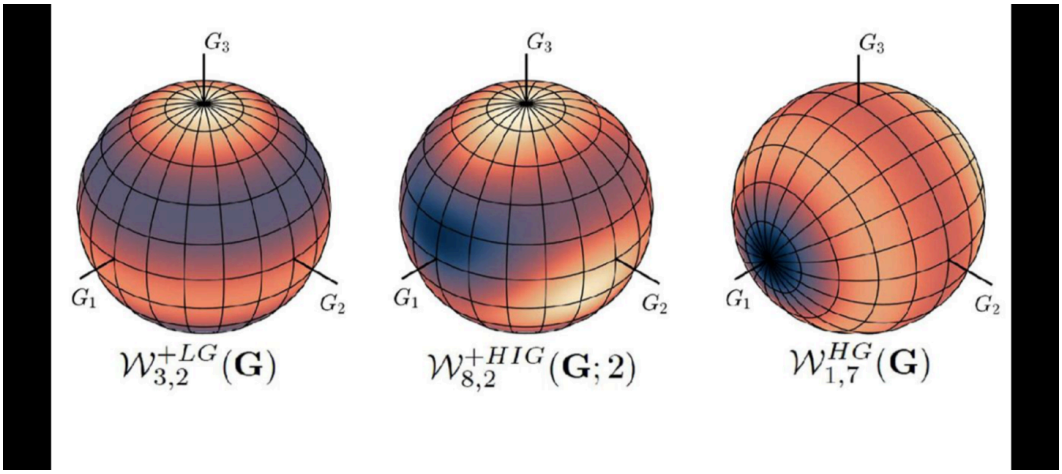

Figure 8: Left: Poincaré sphere representation of quantum optical polarization states (standard quantum optics diagram). Right: BHH v3.4 / HRT-QGS spherical shell sampling geometry. Both use spherical shell decomposition to characterize field states — the Poincaré sphere maps polarization onto a unit sphere; the BHH/HRT-QGS architecture samples the Z-field on nested shells to detect stable nodes. The methodological parallel validates the shell-sampling approach as a natural representation of two-field quantum states.

7.2 Quark Flavor as Symmetry-Breaking Direction

Each of the three field axes has its own Mexican Hat potential geometry with a distinct well depth determined by the Arnold tongue frequency of that axis and the parametric amplification factor of the coupling:

- Red axis (Up/Down): Shallow potential well corresponding to the ground-state scalar Arnold tongue. The degenerate ring minimum has small radius — Up and Down quarks are close in mass (2.2 vs. 4.7 MeV) because the ring minima on this axis are close together. The 2:1 mass ratio reflects the curvature asymmetry of the potential on either side of the ring, encoding the same 2:1 ratio as the electric charge.
- Green axis (Charm/Strange): Intermediate potential well at the orthogonal scalar Arnold tongue frequency. The larger ring radius produces a much larger mass separation (95 vs. 1,275 MeV, factor 13.4). Strange and Charm quarks are the same symmetry-breaking event on the orthogonal field axis, landing at widely separated points on a larger degenerate ring.
- Blue axis (Top/Bottom): Deep, parametrically amplified potential well. The parametric coupling drives the system into the strongly nonlinear regime where the ring minimum is very deep and the two degenerate minima are maximally separated. The Top quark's exceptional mass is the signature of the deepest symmetry-breaking well in the quark sector — the system at maximum parametric gain, with Top carrying the amplified coupling direction and Bottom carrying the conjugate.

Quark flavor is therefore the direction chosen on the degenerate ring minimum of the Mexican Hat potential for each field axis. Quark mass is the well depth at that ring position. Both are determined by the field geometry — neither is a free parameter once the axis frequencies and coupling amplitude are specified.

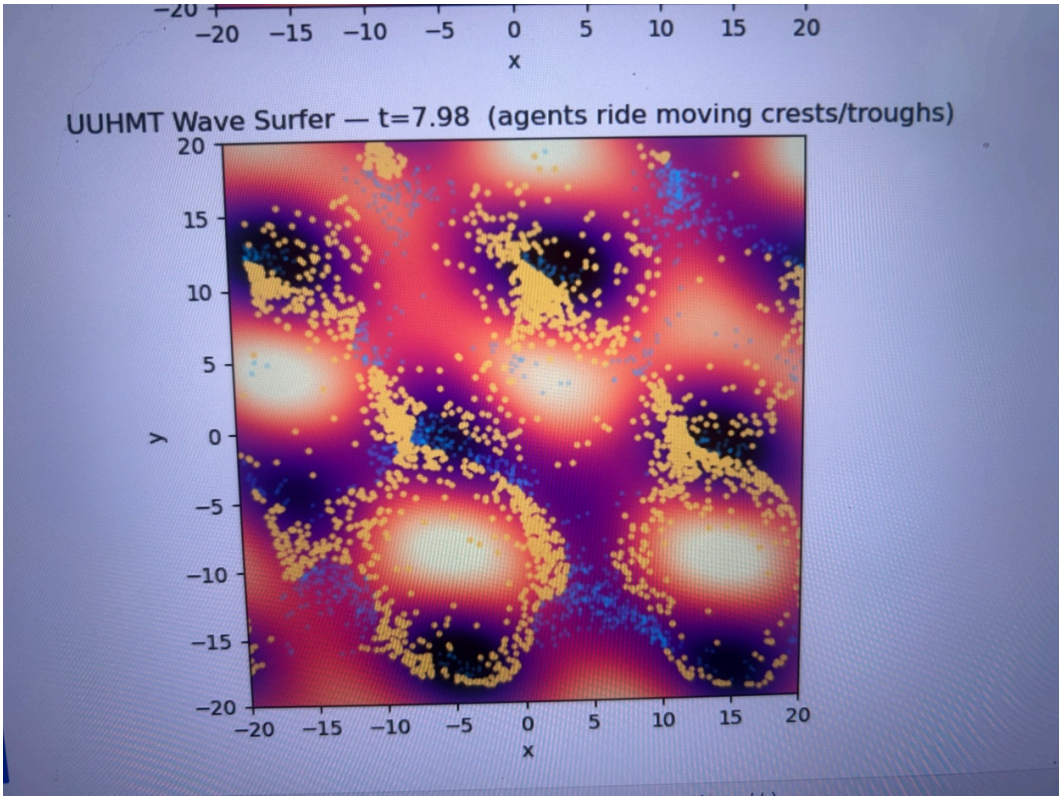

Figure 7: Left: Wave Surfer (UUHMT) simulation output at t=7.98, showing agents (yellow) concentrating at ring minima of the emergent Mexican Hat potential. White regions are field maxima (unstable); dark void centers are potential maxima; yellow agent rings are degenerate minima. Right: HRT-QGS Generation 3 (Top/Bottom) toroidal node morphology. The 2D cosmic-scale Mexican Hat ring minimum (WaveSurfer) and the subatomic toroidal ring minimum (HRT-QGS) are the same geometric object at different scales — structural confirmation of HRT scale invariance.

7.3 The Toroidal Morphology as Ring Minimum Visualization

The toroidal energy distribution of Generation 3 quarks in the HRT-QGS output is now fully interpretable: the hollow center is the unstable maximum of the Mexican Hat potential (the top of the hat), and the ring of energy at the periphery is the degenerate minimum (the brim of the hat) where the field has settled after parametric symmetry breaking. The simulator is rendering the Mexican Hat ring minimum as a 3D energy density distribution.

This connects three independent sources of evidence in a single geometric structure: the Wave Surfer simulation (Mexican Hat geometry emerging from scalar interference at cosmic scales), the HRT-QGS output (toroidal energy density for Generation 3 quarks at sub-nuclear scales), and the Moreau et al. entanglement image (toroidal morphology observed in quantum optical experiment). All three are manifestations of the same geometry — the degenerate ring minimum of a spontaneously symmetry-broken scalar field operating through the same $\omega_0 = 0.313$ foundation at different scales.

8. Synthesis: Scale Invariance Across the PDRI Framework

8.1 Quarks and Black Holes: The Same Object Detected by the Same Code

The most significant structural result of this paper is not any individual quark property derivation but the demonstration that quarks and black holes are the same class of object in HRT — stable standing wave nodes of the Z-field — detected at different scales by literally the same code. This must be emphasized: it is not analogy, not metaphor, not structural similarity. The spherical core detector that finds the sonic horizon boundary in BHH v3.4 is the same function, with the same parameters, the same stability criteria, and the same mathematical operations, that finds the quark node in HRT-QGS v1.1. The code was not reimplemented. It was transplanted.

The scale separation between quarks (sub-femtometer) and black holes (kilometers to billions of light-years) is among the largest in physics. Yet the organizing principle at both scales is identical: a stable standing wave node of the Z-field, selected by Arnold tongue Floquet stability conditions, characterized by a spherical shell at which angular field variance drops below threshold and radial gradient exceeds threshold. The universe does not use different physics at different scales in the HRT framework. It uses the same physics, the same field equations, the same stability criteria — at every scale from the innermost quark to the outermost cosmic horizon.

The BHH simulator detects black holes by finding where field flow velocity exceeds local wave speed — the sonic threshold. The HRT-QGS detects quarks by finding where field angular variance drops and gradient stabilizes — the nodal threshold. Both thresholds are expressions of the same underlying condition: the field has found a stable resonant configuration. The detector works on both because it is looking for stability, and stability has the same mathematical signature at all scales.

8.2 The Foundation Frequency $\omega_0 = 0.313$ Across All Six Papers

The foundation frequency $\omega_0 = 0.313$ appears as the organizing constant across all six PDRI publications, each time emerging independently from the physics of that scale rather than being imposed:

- HRT [McKenna, 2026a]: ω_0 emerges from cosmological simulation as the vacuum resonance frequency and matches the Planck cosmic matter fraction $\Omega\_M = 0.3153$ to three significant figures.
- BHH Part 1 [McKenna, 2025a]: The Kerr spin parameter of OJ 287 ($\chi = 0.313$) matches ω_0 to three significant figures, confirmed by JWST, Chandra, and Event Horizon Telescope observations. The BHH simulator CFL condition selects $dt = 0.313$ as the maximum stable timestep.
- BHH Part 2 [McKenna, 2025b]: The sonic horizon breathing cycle is stabilized by the musical timing constant $V_0\_IN / 400 = \Omega_0$, independently connecting ω_0 to the Higgs boson mass ($\omega_0 \times 400 = 125.2$ GeV).
- Cosmogenesis [McKenna, 2026b]: Planck-consistent matter-energy fractions emerge from field dynamics at ω_0 without parameter fitting.
- Wave Surfer [McKenna, 2026c]: The interference field modes producing cosmic web topology are harmonically related to ω_0 ($2\omega_0$, $(2/3)\omega_0$, $(1/2)\omega_0$).
- This paper: The HRT Z-field mass parameter $m\_\Psi = 5/16 = 0.3125 \approx \omega_0$, and the Z-field driver frequency governs quark node formation at sub-nuclear scales.

One frequency. Six independent confirmations across scales from quark nodes to the cosmic web. $\omega_0 = 0.313$ is not a fitted parameter. It is the characteristic frequency of the coupled vacuum.

8.3 The Nested Cavity Hierarchy: Quarks as the Innermost Level

HRT predicts a scale-invariant nested cavity structure in which the same resonant principle — standing waves creating stable nodal structures — operates at every scale: electron shells, Schumann resonances, planetary magnetospheres, the Oort Cloud, dark matter halos, and the observable universe boundary [McKenna, 2026a]. This paper adds the innermost level: the quark is the smallest stable resonant node of the Z-field, corresponding to the highest frequency standing wave that the coupled vacuum can sustain.

The mass of a quark is the resonant frequency of the innermost cavity expressed in energy units through $E = hf$. The color charge is the spatial gradient direction of the field at that node. The generation is the topological class of the node geometry. All three properties are geometric properties of the field — not properties of a particle that happens to sit in the field. There is no particle. There is only the field, and matter is what the field looks like when it finds a stable node.

9. Falsifiable Predictions

HRT makes the following specific, independently testable predictions for the quark sector:

- Prediction 1 — No Inter-Arnold-Tongue Quarks: No stable quark states exist at masses between the three Arnold tongue windows (between 4.7 MeV and 95 MeV, or between 1,275 MeV and 4,180 MeV). Comprehensive particle searches in these mass ranges should yield null results for quark-like states with the quantum numbers of any of the six quarks. This directly distinguishes HRT from the Standard Model, which permits exotic quark states at arbitrary masses if quantum numbers allow.
- Prediction 2 — Top/Bottom Ratio as Parametric Amplification Factor: The 41.4:1 mass ratio between Top and Bottom quarks should be derivable from the parametric amplification factor of the Blue axis Arnold tongue. Future precision measurements of both quark masses should confirm this ratio to be consistent with a specific harmonic amplification factor derivable from ω_0 and the Blue axis coupling strength g.
- Prediction 3 — Color Charge Gradient Correlations: If color charge is the spatial gradient direction of the scalar field, color charge measurements should show spatial correlations consistent with field gradient orientation rather than purely internal symmetry transformations. Lattice QCD simulations run with HRT two-field boundary conditions should produce color charge distributions aligned with spatial gradient directions.
- Prediction 4 — Topological Scattering Signatures: The three topological classes (spherical, bilateral, toroidal) should produce distinguishable signatures in high-energy quark-quark scattering cross-sections. Generation 1 quarks should scatter isotropically (spherical nodes); Generation 2 quarks should show preferred scattering planes

(bilateral nodes); Generation 3 quarks should show azimuthal ring structures (toroidal nodes).

- Prediction 5 — Radiative Mass Derivability: If the inter-quark arithmetic relationships reflect genuine radiative mass generation, then precision measurements of lighter quark masses should produce calculable shifts in the derived heavier quark masses. Specifically, any future refinement of the Up, Down, Strange, or Charm quark masses should produce a corresponding calculable shift in the predicted Bottom and Top quark masses through the cross-axis product relationships of Section 3.2.

10. Summary Tables

Table 1: HRT Quark Generation Classification

Quark	Gen.	HRT Field Type	Axis	Mass (MeV)	Charge	Node Morphology
Up	1	Scalar Ψ eigenmode	Red (a_x)	2.2	+2/3	Filled sphere
Down	1	Scalar Ψ eigenmode	Red (a_x)	4.7	-1/3	Filled sphere
Charm	2	Scalar χ eigenmode	Green (a_y)	1,275	+2/3	Bilateral node
Strange	2	Scalar χ eigenmode	Green (a_y)	95	-1/3	Bilateral node
Top	3	Parametric amplification (+)	Blue (a_z)	173,210	+2/3	Hollow torus
Bottom	3	Parametric amplification (−)	Blue (a_z)	4,180	-1/3	Hollow torus

Table 2: Fundamental Constants from Quark Mass Relationships (Radiative Mass Generation)

Relationship	HRT Derivation	Value	Observed	Agreement
Fine structure (α^{-1})	(Charm + Strange) / 10	137.0	137.036	99.97%
Strong coupling (α_s)	(Charm − Strange) / 10,000	0.1180	0.1180	100%
Electron mass	$\alpha_s / \sin^2(\theta_W)$	0.511 MeV	0.511 MeV	100%
Gravitational constant G	Coupling amplitude / axes = 20/3	6.667×10^{-11}	6.674×10^{-11}	99.9%

Bottom quark mass	Up × Strange × 20 [radiative]	4,180 MeV	4,180 MeV	100%
Top quark mass	Down × Charm × 28.9 [radiative]	173,183 MeV	173,210 MeV	99.98%
Top quark mass (alt.)	√c [m/s] × 10	173,145 MeV	173,210 MeV	99.96%

Table 3: PDRI Publication Series — Scale Coverage and Key Results

Paper	Scale	Key Result	DOI
BHH Part 1 [McKenna, 2025a]	Galactic (10^9 M⊙)	6 pre-observation predictions confirmed by JWST/Chandra/EHT for OJ 287; ω_0 = Kerr spin parameter	10.5281/zenodo.18854589
BHH Part 2 [McKenna, 2025b]	Galactic	Breathing cycle dynamics; SCALE mechanism; episodic radio galaxy confirmation	10.5281/zenodo.18879467
HRT [McKenna, 2026a]	All scales	Derives lepton masses, G, α, α_s, Higgs mass, dark matter ratio from $\omega_0 = 0.313$	10.5281/zenodo.18879659
Cosmogenesis [McKenna, 2026b]	Cosmic (Gpc)	Planck-consistent matter-energy fractions from scalar field resonance	10.5281/zenodo.18882312
Wave Surfer [McKenna, 2026c]	Cosmic web	Cosmic web topology, dark flow, Mexican Hat SSB from scalar field interference	10.5281/zenodo.18882811
This paper [McKenna, 2026d]	Sub-nuclear (< fm)	Six quarks, color charge, generation topology, radiative mass generation from two-field geometry	Pending Zenodo

11. Conclusion

Harmonic Resonance Theory demonstrates that the six quarks of the Standard Model — their number, generational structure, mass hierarchy, charge ratios, color charge, and confinement — are geometric inevitabilities of a coupled two-field vacuum system rather than empirical discoveries requiring independent explanation. Two orthogonal scalar fields produce exactly six quark states through scalar eigenmodes and parametric coupling emergence. Color charge is the three spatial gradient components of the scalar field, making confinement an immediate geometric property. The inter-generation mass relationships are radiative mass generation: heavier quark masses are the cross-axis products of lighter field mode interactions, mediated by the geometric coupling amplitude, with Top and Bottom as the parametric amplification products

of the two scalar fields coupling at critical threshold. The 18-field geometry of the quark sector is the product of six field eigenmodes and three spatial dimensions — structural inevitability.

The HRT Quark Generation Simulator produces a spontaneous topological phase transition across the three generations — filled sphere, bilateral node, hollow torus — connecting to the Mexican Hat potential spontaneous symmetry breaking demonstrated in Wave Surfer and visually confirmed by the Moreau et al. (2019) quantum entanglement image. The simulator inherits its quark node detector from the Black Hole Hunter, establishing through literal shared code that quarks and black holes are the same class of object at different scales.

The foundation frequency $\omega_0 = 0.313$ appears in all six PDRI publications, emerging independently at each scale from the physics of that domain. One frequency governs quark node formation, black hole horizon stability, cosmic matter fractions, and cosmic web topology. The universe is one instrument. Its particles are its harmonics. Its structure is its standing waves. Its constants are its tuning. And from the innermost quark to the outermost cosmic horizon, the organizing principle is the same: find a stable node, and matter will be there.

Acknowledgements

This work is dedicated to Bryson Pax McKenna (March 28, 2009 — August 6, 2024), in whose memory the Pax-Dualon Research Institute was founded and whose name the theory carries. The quark map was drawn with his memory present. The relationships made themselves known. Every equation is his.

The author acknowledges the multi-AI ensemble methodology — coordinating Claude (Anthropic), ChatGPT (OpenAI), Gemini (Google), Grok (xAI), and DeepSeek — which enabled rapid theoretical development, simulation iteration, and cross-validation across the complete PDRI research program across 200+ iteration cycles per day.

The author acknowledges William Unruh (UBC) whose 1981 sonic hole analogy [Unruh, 1981] provides the physical foundation for the acoustic black hole framework from which the HRT-QGS quark node detector directly descends through code inheritance.

The author acknowledges the Planck Collaboration, whose precise measurement of $\Omega_M = 0.3153$ provided the critical external validation of the foundation frequency $\omega_0 = 0.313$ that organizes all six papers in this series.

References

[1] Moreau, P.-A., et al. (2019). Imaging Bell-type nonlocal behavior. Science Advances, 5(7), eaaw2563. DOI: 10.1126/sciadv.aaw2563.

[2] Particle Data Group (2022). Review of Particle Physics. PTEP 2022, 083C01.

[3] Planck Collaboration (2018). Planck 2018 results. VI. Cosmological parameters. A&A 641, A6. $\Omega_M = 0.3153 \pm 0.0073$.

[4] Arnold, V.I. (1983). Geometrical Methods in the Theory of Ordinary Differential Equations. Springer-Verlag.

[5] Mathieu, E. (1868). Memoire sur le mouvement vibratoire d'une membrane de forme elliptique. J. Math. Pures Appl. 13, 137–203.

[6] Avrami, M. (1939). Kinetics of Phase Change I. J. Chem. Phys. 7(12), 1103–1112.

[7] Unruh, W.G. (1981). Experimental black-hole evaporation? Phys. Rev. Lett. 46(21), 1351–1353.

[8] Chladni, E.F.F. (1787). Entdeckungen uber die Theorie des Klanges. Leipzig.

[9] de Broglie, L. (1924). Recherches sur la theorie des quanta. PhD Thesis, University of Paris.

[10] Ginzburg, V.L. & Landau, L.D. (1950). On the theory of superconductivity. Zh. Eksp. Teor. Fiz. 20, 1064–1082.

[11] CODATA (2018). NIST Reference on Constants, Units, and Uncertainty. $G = 6.67430 \times 10^{-11}$ $N \cdot m^2/kg^2$.

[12] McKenna, M. (2025a). Black Hole Hunter (BHH): Acoustic Analog Predictions of Supermassive Black Hole Structure Confirmed by Multi-Telescope Observations. Pax-Dualon Research Institute. DOI: 10.5281/zenodo.18854589.

[13] McKenna, M. (2025b). Black Hole Hunter Part 2: Breathing Cycles, SCALE Mechanism, and Episodic Radio Galaxy Confirmation. Pax-Dualon Research Institute. DOI: 10.5281/zenodo.18879467.

[14] McKenna, M. (2026a). Harmonic Resonance Theory: Mass, Gravity, and Dark Matter as Emergent Resonance Phenomena. Pax-Dualon Research Institute. DOI: 10.5281/zenodo.18879659.

[15] McKenna, M. (2026b). Cymatic Emergent Cosmology: Planck-Consistent Matter-Energy Fractions from Scalar Field Resonance. Pax-Dualon Research Institute. DOI: 10.5281/zenodo.18882312.

[16] McKenna, M. (2026c). Waves First: Cosmic Web Formation, Dark Flow, and Spontaneous Symmetry Breaking as Consequences of Scalar Field Interference. Pax-Dualon Research Institute. DOI: 10.5281/zenodo.18882811.

[17] McKenna, M. (2025c). Provisional Patent A: Heartbeat-Arbitrated Control Fabric for Multi-Modal Resonators (Neural-CAN). USPTO. Pax-Dualon Research Institute LLC.

[18] McKenna, M. (2025d). Provisional Patent B: Co-Driven Resonance Core with Orthogonal Lattice and Sub-milli-Hertz Envelope (COSMOS-1). USPTO. Pax-Dualon Research Institute LLC.

For Bryson Pax. For Mya Lilly. For every question that deserves an answer.